Chapter 8

ACTIVATION MEASUREMENTS FOR THERMAL NEUTRONS

Part J. Evaluation of Thermal Neutron Transmission Factors

Stephen D. Egbert

Introduction

In order to relate thermal neutron activation measurements in samples to the calculated free-in-air thermal neutron activation levels given in Chapter 3, use is made of sample transmission factors. Transmission factors account for the modification of the fluence and activation at each sample's *in situ* location. For the purposes of this discussion, the transmission factor (TF) is defined as the ratio of the *in situ* sample activation divided by the free-in-air (FIA) activation at a height of 1 m above ground at the same ground range. The procedures for calculation of TF's and example results are presented in this section.

Parameters Affecting Thermal Neutron Transmission Factors

Transmission factors for thermal neutrons are affected by several parameters:

1. sample height,
2. shielding of the sample by surrounding sample material,
3. shielding by other nearby structures or objects,
4. neutron energy activation cross section for the isotope or isotopes that produce the measured isotope, and
5. compositions of the sample materials.

At Hiroshima and Nagasaki, most samples are near the surface with no line-of-sight shielding in the direction toward the burst point of the bomb. The materials comprising the samples usually do not have neutron properties extremely dissimilar from soil or concrete. For such samples, a TF of 1.0 can be used as an initial approximation, but with a large uncertainty of about 20%. This can be improved by using a more detailed model of the sample's location. Modeling of the

sample is even more important when any of the parameters significantly affect the TF, such as for concrete cores or granite samples. In this section, sample-specific TFs are presented for the ^{36}Cl samples. TFs for some ^{152}Eu and ^{60}Co samples are also presented if geometries and material details are known. For samples that are not well described, default TFs will be suggested from among these sample-specific calculations. Both the calculated and default TFs will be used in the following comparisons between calculations and measurements.

The parameters that affect the TFs are briefly discussed here. An increase in the height of the sample, for example, generally decreases the thermal neutron activation in the sample. Although it moves the sample closer to the exploding bomb, raising the height takes the sample farther from the ground, which is a large source of thermal neutrons. The air is a poor source of thermal neutrons because nitrogen has a large thermal neutron absorption cross section and air has a small hydrogen fraction. The thermal FIA activation decreases by about 1% for every 1 m increase in height above a concrete or dry ground surface. Above wet soil the height effect is slightly more important, 1.5% decrease for each meter. If the sample itself is a significant source of thermal neutron fluence, this effect will be reduced.

If shielding material is placed between the sample and the radiation source the thermal neutron TF will often decrease. This is especially true for shielding materials such as granite that have low hydrogen content like the air. On the other hand, shielding materials with a significant amount of hydrogen, like wet soil, have almost a doubling in activation at a depth of 2-4 cm compared to that at a height of 1 m above ground. For a typical shielding material sample like concrete, at a depth of 1 cm there is about a +15% increase in activation compared to that at the surface for a height of 1 m above concrete. This holds true at all ground ranges. The magnitude of this increase will depend on the amount of moisture and absorptive isotopes in the concrete or sample material.

Replacing the 50-cm thick ground with concrete also reduces the thermal activation at a height of 1 m by about 15%. Figure 1, which is the result of an air-over-concrete calculation for Hiroshima, shows many of the effects described for thermal neutron activation of ^{36}Cl. It is noteworthy that the shielding by concrete and effect of moisture in concrete seem to cancel each other out at 1-cm depth into the concrete. The activation at that depth is the same as at the standard height of 1 m above ground for the neutron activation values given in Chapter 3 (i.e., a TF of approximately 1.0).

The thermal and epithermal neutron energy responses of the ^{35}Cl(n,γ), ^{40}Ca(n,γ), ^{62}Ni(n,γ), and ^{151}Eu(n,γ) reactions are similar in shape and result in the same TF. The energy responses of the activation cross sections for the ^{59}Co(n,γ) and ^{153}Eu(n,γ) reactions are somewhat different. Table 1 shows thermal and epithermal activation cross sections for each of these reactions and the ratio between them. The ^{59}Co and ^{153}Eu reactions are more sensitive to the *in situ* epithermal fluence. Typically this can make about a 5% difference in TF for these isotopes compared with the previous ones, which are closer to 1/v in shape, where v is the neutron velocity.

The thermal neutron TF depends on the fraction of hydrogen and thermal neutron absorbers in the sample material composition. Nearby structures such as buildings, trees, vehicles, and pavement will also have an effect on the activation. For example, tree foliage will moderate the incident fluence, causing an increase in thermal neutron activation near the surface and a decrease in the activation at depth. Trace neutron elements, like gadolinium, absorb thermal neutrons diffusing through the sample, decreasing the activation at depth. However, they typically have only a small effect on the TF for surface samples (Chapter 10, Part C).

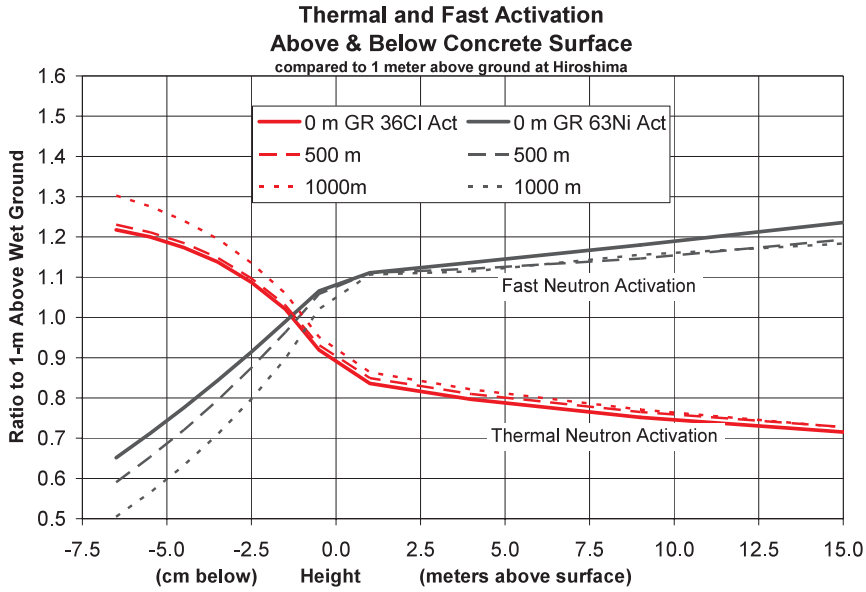

Figure 1. *Thermal $^{35}Cl(n,\gamma)^{36}Cl$ and fast activation $^{63}Cu(n,p)^{63}Ni$ above and into concrete compared to 1 m above Hiroshima wet soil.*

Table 1. Thermal and epithermal neutron cross sections for reactions producing measured activation products[a]

Cross section (barns)	Thermal 2200 m/s	Epithermal resonance integral	Ratio (thermal/fast)
^{35}Cl	43.6	18.0	2.4
^{40}Ca	0.41	0.22	1.9
^{59}Co	37.2	74.0	0.5
^{62}Ni	14.5	6.6	2.2
^{151}Eu	5900.	1510.	3.9
^{153}Eu	312.	1420.	0.2

[a]See (Mughabghab et al. 1981, 1984)

A typical concrete or granite TF for thermal neutron activations in near-surface samples can be estimated by combining effects from the five parameters described above:

1. height effect at 5 m = ~0.95,
2. buildup in concrete at 1-cm depth = ~1.15 (and ~1.00 for granite),
3. concrete surfaces on ground = ~0.85,
4. isotope response = ~1.0, and
5. trace neutron absorbers = ~0.98.

Hence, the TF for a near-surface concrete sample is about $0.95 \times 1.15 \times 0.85 \times 1.0 \times 0.98$ or about 0.9, and the TF for a near-surface granite sample is about $0.95 \times 1.00 \times 0.85 \times 1.0 \times 0.98$ or about 0.8. For core samples, activation decreases about an order of magnitude for every 30 cm of depth, after the thermal neutron buildup thickness of about 10 cm.

Each sample is unique in range, geometry, and material composition; thus, specific shielding situations will give a unique TF for each sample. In order to improve the TF and reduce uncertainty, TFs have been calculated for as many samples as possible. This was done at their originally reported distances. Recently the sample locations have been more accurately located using new maps and aerial photographs. Also, a new DS02 hypocenter location has been adopted. These changes cause an adjustment of up to 20 m in sample distances at Hiroshima and a few meters at Nagasaki. The TF, being a ratio, is not sensitive to these small changes in distance, and the TF calculated at the original reported distance is valid for both the DS86 and DS02 hypocenter locations.

Determination of Sample-Specific Transmission Factor

The calculations of ^{36}Cl and other isotopes activated by thermal neutrons in concrete and granite samples were performed using the Monte Carlo Adjoint Shielding Code System (MASH) (Johnson 1999). This is the same methodology used for both DS86 and DS02. The code is ideal for situations in which a shielded sample point is exposed to a large field of incident neutrons. The adjoint method starts neutrons at the sample point in proportion to the activations response and runs them backwards in space and time to exit a closed surface that surrounds the sample and any surrounding shielding. The leaking particles are weighted according to the incident fluence they meet coming into the surface. The weights are added and the result is normalized to give the activation in the sample.

Geometry Model. The shielding around the sample point is modeled using a combination of primitive bodies, like boxes and ellipsoids. For each of the samples, geometric models consisting of about ten primitive bodies are constructed. The important aspects of the geometry are the detector point and building height, the incident angle, and any shielding between the detector point and the direction of the main source (i.e., the bomb). For thermal neutron activation, structures not in the line-of-sight must be included when they may block or change the scattering portion of the incident fluence.

Sample-specific TFs have been calculated for the ^{36}Cl measurements of Straume et al. (Chapter 8, Part D). These samples are listed in Table 2. Except for where it is noted that an alternative model was used, customized geometry models were constructed for the samples. Table 3 lists other specific samples, which were modeled and calculated for the ^{36}Cl measurements of Rühm et al. (Chapter 8, Part E) and Nagashima et al. (Chapter 8, Part F). Also, included in this table is the TF for a generic gravestone model. Finally, the TFs calculated for a somewhat limited number of ^{60}Co measurements by Hashizume et al. are listed in Table 4 (Chapter 8, Part A).

Illustrations of all of the exposure geometries used in these various sample TF calculations are shown in Figures A1-A33 of Appendix A. They were all calculated at their originally reported distances. The information about the geometries and material constituents came from several sources. Dr. Fujita (Fujita 1990-2002) at RERF sent to Dr. Straume and other measurers

drawings, photographs, and descriptions of many of the samples. These were passed along to Science Applications International Corporation who simplified the information into the illustrated models. For other specific samples, such as the published ^{60}Co results of Dr. Kerr (Kerr 1985) and Dr. Maruyama (Maruyama 1987), the published reports were the basis for modeling.

Table 2. Sample IDs of Straume, location, material type and distance to DS02 hypocenter. Unless noted, the geometry model was customized for each sample

Sample ID#	Sample location	Sample material	Distance from hypocenter (m)
S-108	Motoyasu Bridge Railing	Motoyasu Granite (core)	134
S-67	Motoyasu Bridge Pillar	Motoyasu Granite (core)	128
S-23	Hiroshima Bank	City Hall Concrete (surface)	257
S-28	Aioi Bridge	Motoyasu Granite (surface)	257
S-69	Gokoku Shrine	Gokoku Concrete (core)	388
S-120	Gokoku Shrine	Fukoku Granite (core)	388
S-66	Shirakami Shrine	Shirakami Granite (core)	487
S-109	Shirakami Fence[a]	Gravestone Granite (surface)	504
S-1	Chugoku Electric Co.	Chugoku Concrete (surface)	670
S-65	Kirin Beer Hall	Kirin Concrete (core)	679
S-111	Myochoji[a]	Gravestone Granite (surface)	639
S-112	Old Prefecture Office[a]	Gravestone Granite (surface)	877
S-110	Honkeiji[a]	Gravestone Granite (surface)	896
S-24	Old Prefecture Office[a]	Gravestone Granite (surface)	877
S-113	Enryuuji[a]	Gravestone Granite (surface)	925
S-114	Shingyoji[a]	Gravestone Granite (surface)	915
S-14	Hiroshima City Hall	City Hall Concrete (core)	1060
S-116	Kozenji[a]	Gravestone Granite (surface)	1177
S-70	HU Elementary School	Elementary Concrete (core)	1277
	Ono Oil Shop	Granite (estimate TF)	1291
S-58	Teishin Hospital	City Hall Concrete (core)	1375
S-6	HU, Main Bldg.[b]	Elementary Concrete (core)	1386
S-80	HU Radioisotope[b]	Elementary Concrete (core)	1466
S-59	Red Cross Hospital	Red Cross Concrete (core)	1474
S-60	Red Cross Hospital	Red Cross Concrete (core)	1474
S-76	Red Cross Hospital	Red Cross Concrete (core)	1501
S-46	Postal Savings	Red Cross Concrete (core)	1591
S-47	Postal Savings	Red Cross Concrete (core)	1600
S-62	Misasa Bank[c]	Red Cross Concrete (core)	1682
	Nagasaki University Hospital	Nagasaki University Hospital	653
	Mitsubishi Arms and Steel Works[d]	Nagasaki University Hospital	1075
	Fuchi Middle School[d]	Nagasaki University Hospital	1156

[a]Gravestone model used.
[b]HU Elementary School model used.
[c]Postal Savings Building model used.
[d]Nagasaki University model used with sample specific building orientation.

There are many models described in the DS86 Final Report, Vol. 2, Chapter 4 Appendix 11, which are used in this work also (Kaul 1986). Two sources were extremely helpful. The *US Strategic Bombing Survey* (USSBS 1947) and the *Architectural Witness to the Atomic Bombing* (Hiroshima Peace Memorial Museum 1996) contained many drawings and pictures of structures throughout the whole city of Hiroshima.

Table 3. Location, material type and distance to DS02 Hiroshima hypocenter of other ^{36}Cl samples. Unless noted, the geometry model was customized for each sample

Investigator	Sample location	Sample material	Distance from hypocenter (m)
Rühm	Saikoji Grave	Saikoji Granite core	94
Hoshi	Suiseko River Abatement	Motoyasu Granite core	~380
Rühm	Faculty of Science Wall Cores & Stone Gutters	Faculty of Science Concrete & Faculty of Science Granite	1384-1391
Rühm	Postal Savings	Postal Savings Granite	1591
Rühm	Generic Graveyard	Gravestone Granite	0 to 2000

Table 4. Location, material type and distance to DS02 Hiroshima hypocenter of ^{60}Co samples. Unless noted, the geometry model was customized for each sample

Investigator	Sample location	Sample material	Distance from hypocenter (m)
Hashizume	Chiyoda Seimei (Life Insurance) Building	City Hall Concrete & Rings	~116
Hashizume	Hiroshima Chamber of Commerce and Industry	City Hall Concrete & Rings	~237
Hashizume	Hiroshima Bank	City Hall Concrete & Rebar	257
Hashizume	Fukoku Seimei (Life Insurance) Building	City Hall Concrete & Rings	~325
Hashizume	Honkawa Primary School	City Hall Concrete & Rings	408
Hashizume	Fukuromachi Primary School	City Hall Concrete & Rings	468
Hashizume	Sentry Box	City Hall Concrete & Rebar	683
Hashizume	Kirin Beer Hall	City Hall Concrete & Rings	690
Hashizume	Kodokan	City Hall Concrete & Rings	748
Hashizume	Water Trough	City Hall Concrete & Rebar	779
Hashizume	Hiroshima City Hall	City Hall Concrete & Rings	998
Hashizume	Powder Magazine	City Hall Concrete & Rebar	1178

Materials. The building and sample materials can play a role in the calculation. The materials chosen for the calculations are specific to the building and sample. If the elemental constituents have been determined, then the calculations use that material for the TF calculations. If there is not a measurement of the elemental composition, another building's material is used. When important trace elements are unknown, a typical amount is added to the material.

The material used for the shielding in each calculation is identified in Tables 2 through 4. The source of information about the elemental composition for each material is provided in Table 5. The composition of each material is given in Table 6, and the atomic density of each element or isotope of the material is given in Table 7.

Table 5. Material types used in calculations and source for element composition

Sample material	Density g/cc	Source of element composition
Gokoku Concrete	2.3	Galbraith Laboratories Report (2000-2001)
Kirin Concrete	2.3	Galbraith Laboratories Report (2000-2001)
City Hall Concrete	2.3	Galbraith Laboratories Report (2000-2001)
Elementary Concrete	2.3	Galbraith Laboratories Report (2000-2001)
Red Cross Concrete	2.3	Galbraith Laboratories Report (2000-2001)
Chugoku Concrete	2.3	Kerr et al. (1990)
Faculty of Science Concrete	2.3	Chapter 8, Part G
Fukoku Concrete	2.191	Nakanishi et al. (1987)
Faculty of Science Granite	2.6	Chapter 8, Part G
Postal Savings Granite	2.6	Chapter 8, Part G
Saikoji Gravestone Granite	2.6	Rühm (1993)
Fukoku Granite	2.693	Nakanishi et al. (1987)
Motoyasu Granite	2.64	Hasai et al. (1987)
Shirakami Granite	2.60	Shizuma et al. (1997)
Water	1.0	
Hiroshima Air	1 atm	Kerr et al. (1987)
Hiroshima Soil	1.7	Kerr et al. (1987)
Iron	7.86	Weast (1976)
Copper	8.94	Weast (1976)

Table 6. Density of mineral compounds (weight fraction) and trace elements (ppm) used in shielding calculations

	Mol. Weight	Gokoku Shrine Concrete	Kirin Hall Concrete	City Hall Concrete	Elementary School Concrete	Red Cross Hospital Concrete	Chugoku Building Concrete	Faculty of Science Concrete	Fukoku Building Concrete	Faculty of Science Granite	Postal Savings Granite	Saikoji Gravestone Granite	Fukoku Building Granite	Motoyasu Pillar Granite	Shirakami Shrine Granite
Ash		0.9365	0.9349	0.9450	0.9569	0.9362		0.9500		0.9900	0.9900	0.9944			
H2O	18.02	0.0635	0.0651	0.0550	0.0431	0.0638		0.0500		0.0100	0.0100	0.0056			.0074-.0092
Na2O	61.98	0.0221	0.0176	0.0210	0.02180	0.0188		0.0177		0.0335	0.0343	0.0377			.0343
MgO	40.31	0.0097	0.0127	0.0091	0.00800	0.0069		0.0082		0.0018	0.0040	0.0044			.0037
Al2O3	101.96	0.1202	0.1015	0.1191	0.12840	0.0999		0.0884		0.1290	0.1340	0.1433			.1350
SiO2	60.08	0.7888	0.7480	0.7738	0.77030	0.6753		0.6950		0.7610	0.7350	0.7130			.7320
SO3	80.06	0.0014	0.0020	0.0017	0.00220	0.0006									.0002
K2O	94.20	0.0278	0.0214	0.0293	0.03230	0.0278		0.0213		0.0046	0.0043	0.0302			.0396
CaO	56.08	0.0890	0.1185	0.0941	0.07640	0.1082		0.0902		0.0109	0.0148	0.0295			.0171
TiO2	79.95	0.0028	0.0035	0.0029	0.00340	0.0028		0.0026		0.0009	0.0017	0.0030			.0002
Fe2O3	159.69	0.0212	0.0374	0.0265	0.02910	0.0239		0.0250		0.0129	0.0189	0.0392			.0279
P2O5	141.94	0.0010	0.0011	0.0008	0.00090	0.0640		0.0005		0.0001	0.0002				
SUM		1.0840	1.0637	1.0783	1.0728	1.0282		0.9489		0.9546	0.9472	1.0003			.9907
Trace Elements ppm															
Al	26.98		6130												
B	10.81	8.1	6.8	4.4	4	5						3.1		<30	
Ba	137.34	263	172	204	337							931			
Be	9.01	5	5	5	5										
Ca	40.08														
Cd	112.40	1	1	1	1	1								0.046	
Cl	35.45	40	20	31	36	20		238		64	87	70			
Co	58.93	14	26	28	10										
Cr	51.99	30	28	14	17										
Cu	63.54	26	31	18	47										
Fe	55.85	8280													
Ga	69.72	28	24	22	30	5									
Li	6.94	11	20	0.4	19	5		26		32	88	50.3		51	
Mg	24.31	975	1652	535	774										
Mn	54.94	314	513	392	434										
Mo	95.95	5	5	5	5										
Ni	58.71	5	10	5	5										
P	30.97	221	153	149	242										
Pb	207.21	5	5	5	5										
Sn	118.70	5	5	5	5										
Sr	87.63	174	152	155	225										
Ti	47.95	1318	1354	1146	1407										
V	50.94	32	39	28	38										
Zn	65.37	33	47	43	39										
Zr	91.22	40	31	36	46										
Sm	150.35	*2.7**	*4.9**	*4.4**	*4.3**	*4**	*4**	2	*4**	4.1	10.2	4.92	*4**	4.2	*4**
Eu	151.96	*0.5**	*0.5**	*0.5**	*0.5**	*0.5**	*0.5**	0.38	*0.5**	0.52	0.46	1.43	*0.5**	0.95	*0.5**
Gd	157.26	2.7	4.9	4.4	4.3	*4**	*4**	2.4	*4**	4	9.9	4.8	*4**	7.1	*4**
Dy	162.50	*2.7**	*4.9**	*4.4**	*4.3**	*4**	*4**	*2.4**	*4**	*4**	*9.9**	*4.8**	*4**	6.6	*4**
Equiv Cd	112.40	43.2	77.9	70.0	68.4	63.7	63.7	37.7	63.7	63.9	157.1	77.8	63.7		63.7

*In italics indicates value is estimated by author (trace elements were set proportional to measured Gd). Values in boxes are measured quantities.

Table 7. Atomic density of isotopes used in shielding calculations (atom/barn/cm)

Element Isotope	DABL B6.3 ID#	Gokoku Shrine Concrete	Kirin Hall Concrete	City Hall Concrete	Elementary School Concrete	Red Cross Hospital Concrete	Chugoku Building Concrete	Faculty of Science Concrete	Fukoku Building Concrete	Faculty of Science Granite	Postal Savings Granite	Saikoji Gravestone Granite	Fukoku Building Granite	Motoyasu Pillar Granite	Shirakami Shrine Granite
H	225	9.77-3	1.00-2	8.46-3	6.63-3	9.81-3	7.69-3	7.69-3	6.06-3	1.74-3	1.74-3	9.74-4	3.63-4	1.04-3	1.45-3
Li-6	309	1.63-7	2.96-7	5.92-9	2.81-7	7.41-8	9.13-7	3.85-7		5.36-7	1.47-6	8.42-7			
Li-7	317	2.03-6	3.70-6	7.39-8	3.51-6	9.24-7	1.15-5	4.80-6		6.68-6	1.84-5	1.05-5			
Be	61	7.68-7	7.68-7	7.68-7	7.68-7		2.46-7								
B-10	39	2.05-7	1.72-7	1.12-7	1.01-7	1.27-7	5.12-7	0.00+0		0.00+0	0.00+0	8.88-8			
B-11	47	8.33-7	6.99-7	4.52-7	4.11-7	5.14-7	2.05-6	0.00+0		0.00+0	0.00+0	3.60-7			
O	415	4.42-2	4.36-2	4.37-2	4.34-2	4.39-2	4.79-2	4.35-2	3.74-2	5.00-2	4.96-2	4.77-2	4.99-2	4.90-2	4.85-2
Na	355	8.53-4	6.91-4	8.23-4	8.69-4	7.65-4	1.10-3	7.92-4	5.08-4	1.68-3	1.74-3	1.89-3	1.86-3	2.01-3	1.73-3
Mg	325	2.88-4	3.84-4	2.74-4	2.45-4	2.16-4	2.62-4	2.82-4		6.95-5	1.56-4	1.70-4		2.40-5	1.40-4
Al	1	2.82-3	2.42-3	2.84-3	3.11-3	2.47-3	3.24-3	2.40-3	1.74-3	3.94-3	4.13-3	4.38-3	4.12-3	4.24-3	4.15-3
Si	505	1.57-2	1.52-2	1.56-2	1.58-2	1.42-2	1.38-2	1.60-2	9.62-3	1.97-2	1.92-2	1.85-2	2.04-2	1.96-2	1.91-2
P	423	1.69-5	1.89-5	1.40-5	1.57-5	1.14-3	1.12-5	9.77-6		2.19-6	4.43-6			1.21-3	
S		2.09-5	3.04-5	2.58-5	3.40-5	9.45-6									
Cl	105	1.56-6	7.81-7	1.21-6	1.41-6	7.81-7		9.30-6		2.83-6	3.84-6	3.09-6			
K	301	7.06-4	5.53-4	7.55-4	8.47-4	7.44-4		6.27-4	6.53-4	1.51-3	1.44-3	9.98-4	1.74-3		1.31-3
Ca	91	1.90-3	2.57-3	2.04-3	1.68-3	2.43-3	1.65-3	2.23-3	8.54-3	3.03-4	4.15-4	8.19-4	2.92-4	5.20-4	4.70-4
Ti	531	4.19-5	5.33-5	4.40-5	5.25-5	4.42-5	4.30-5	4.51-5	2.01-5	1.66-5	3.40-5	5.84-5	2.07-5	4.00-5	3.90-5
V	569	8.70-7	1.06-6	7.61-7	1.03-6		8.43-7								
Cr-50	131	3.44-8	3.22-8	1.61-8	1.95-8		3.90-8								
Cr-52	139	6.69-7	6.25-7	3.12-7	3.79-7		7.59-7								
Cr-53	147	7.63-8	7.12-8	3.56-8	4.33-8		8.65-8								
Cr-54	155	1.90-8	1.78-8	8.88-9	1.08-8		2.16-8								
Mn	333	7.92-6	1.29-5	9.88-6	1.09-5		1.13-5		1.08-5				8.23-6	8.70-6	1.50-5
Fe-54	187	1.85-5	3.32-5	2.34-5	2.62-5	2.20-5	2.34-5	2.53-5	1.83-5	1.46-5	2.17-5	4.45-5	1.55-5	2.64-5	2.59-5
Fe-56	195	2.91-4	5.23-4	3.69-4	4.13-4	3.46-4	3.69-4	3.98-4	2.87-4	2.31-4	3.41-4	7.01-4	2.45-4	4.15-4	4.08-4
Fe-57	203	6.96-6	1.25-5	8.82-6	9.86-6	8.27-6	8.82-6	9.51-6	6.87-6	5.51-6	8.15-6	1.67-5	5.84-6	9.92-6	9.76-6
Fe-58	215	1.05-6	1.88-6	1.33-6	1.49-6	1.25-6	1.33-6	1.43-6	1.04-6	8.30-7	1.23-6	2.52-6	8.81-7	1.50-6	1.47-6
Ni-58	369	8.05-8	1.61-7	8.05-8	8.05-8		5.96-8							9.01-7	
Ni-60	377	3.08-8	6.16-8	3.08-8	3.08-8		2.28-8								
Ni-61	385	1.34-9	2.68-9	1.34-9	1.34-9		9.90-10								
Ni-62	393	4.24-9	8.48-9	4.24-9	4.24-9		3.14-9								
Ni-64	401	1.07-9	2.13-9	1.07-9	1.07-9		7.89-10								
Cu-63	163	3.92-7	4.67-7	2.71-7	7.08-7		3.32-7								
Cu-65	171	1.75-7	2.09-7	1.21-7	3.17-7		1.48-7								
Ga	219	5.56-7	4.77-7	4.37-7	5.96-7	9.93-8									
Sr		2.75-6	2.40-6	2.45-6	3.56-6										
Zr	607	6.07-7	4.71-7	5.47-7	6.99-7		4.80-7								
Mo	341	7.22-8	7.22-8	7.22-8	7.22-8										
Cd	99	1.23-8	1.23-8	1.23-8	1.23-8	1.23-8	2.09-8								
Cd(eqv)	99	5.33-7	9.60-7	8.63-7	8.43-7	7.85-7	7.85-7	4.64-7		8.90-7	2.19-6	1.08-6		9.01-7	8.87-7
Sn	513	5.84-8	5.84-8	5.84-8	5.84-8										
Ba	55	2.65-6	1.73-6	2.06-6	3.40-6		4.24-6					1.06-5			
Pb-206	437	7.89-9	7.89-9	7.89-9	7.89-9		3.94-8								
Pb-207	443	*7.55-9*	*7.55-9*	*7.55-9*	*7.55-9*		3.77-8								
Pb-208	449	*1.75-8*	*1.75-8*	*1.75-8*	*1.75-8*		8.73-8								

Transport Cross Sections. The neutrons were transported through the materials using ENDF/B-VI cross sections (McVane et al. 1995) in the DABL69 energy-group format (Ingersoll et al. 1995; White et al. 2000). The cross-section library does not contain data for some of the key trace elements such as samarium, europium, gadolinium and dysprosium. These elements have very large thermal neutrons cross sections, absorbing a significant portion of thermal neutrons, although they are present in only trace amounts. They are referred to as trace element poisons. The cross sections for these poisons are given in Table 8. The contributions of these four trace elements to the absorption cross sections were accounted for by adding an equivalent amount of cadmium. Cadmium was chosen rather than boron, because its thermal to epithermal absorption cross-section ratio is similar to that of a typical mixture of these trace elements poisons (4, 0.5, 4, and 4 ppm for Sm, Eu, Gd, and Dy, respectively). The thermal neutron absorption of the typical mixture of the trace neutron poisons is obtained with about 63.7 ppm of cadmium.

Table 8. Thermal and epithermal neutron cross sections for trace elements poisons

Cross section (barns)	Thermal cross section 2200 m/s	Epithermal resonance integral	Ratio (thermal/epithermal)
B	767.	344.	2.23
Cd	2520.	70.	36.
Sm	5670.	1400.	4.1
Eu	4565.	2320.	2.0
Gd	48890.	390.	125.4
Dy	940.	1480.	0.6
4 / 0.5 / 4 / 4 ppm of Sm/Eu/Gd/Dy			15.8

Fluences. The unperturbed air-over-ground neutron fluences are obtained from discrete ordinate calculations of both the prompt and delayed neutron fluences described in Chapter 3. They are given in angle and energy bins at every 25 m from the hypocenter. Values are obtained by interpolations at locations between the radial meshes.

Responses. The thermal neutron responses described in Table 1 are derived from ENDF/B-VI cross sections. They were converted from fine multigroup data, described in Chapter 3 to the DABL69 energy-group structure (Ingersoll et al. 1989) by collapsing with representative neutron spectra for Hiroshima at a height of 1 m above ground. It is important to note that ^{36}Cl is also produced via a fast neutron reaction, ^{39}K(n,α)^{36}Cl, which has an energy threshold of about 1 MeV. Its cross section is found in the JENDL-3 cross-section library (Shibata 1990). Interestingly, a thermal neutron reaction cross section at 2,200 m s^{-1} is given as 4.3 millibarn. The fast neutron cross-section data does not begin until 1 MeV. With the given Q-value and Coulomb barrier it is quite unlikely, however, that the thermal cross section is that large. The cross section was remeasured several years ago and found to have an upper limit of 0.164 millibarn (Krauthan 1988; Rühm 2000). The amount of thermal activation from ^{39}K(n,α)^{36}Cl is clearly not well known. However, even at its maximum, it is a small portion of the activation from ^{39}K, which itself is a small portion of the total ^{36}Cl production, and will not contribute much uncertainty to

the calculation.

Most of the ^{36}Cl is produced by the $^{35}Cl(n,\gamma)$, reaction. The fast–neutron reaction $^{39}K(n,\alpha)^{36}Cl$ adds a small portion to the total activation. At farther distances in Hiroshima, this becomes a more significant fraction of the total. For example, it contributes less than 1% of the neutron activation at ground ranges of 400 m or less. However, at ground ranges beyond 1,000 m, it can account for more than 10%. This is due to the rapid and continual hardening of the Hiroshima neutron spectrum during air transport.

Coupling. Each adjoint neutron particle that escapes the enclosing surface is scored, and its weight is multiplied by the neutron fluence corresponding to its energy and angle. This gives an activation response at the adjoint starting point from the incident fluence estimated by one neutron path. This is repeated many times, selecting neutron paths randomly according to probabilities associated with the material cross sections. The contributions from all the escaping neutrons are averaged to give the in-situ activations at the sample point. The TF is calculated from the ratio of the *in situ* calculated activation divided by the free-in-air activation at a height of 1 m above ground at the same ground range.

Results. The TFs from the DS02 sample-specific modeling calculations are given for several relevant isotopes. The TFs were calculated at the recorded sample depth, if there was only one measurement for that geometry model. For deeper cores, calculations were made at every 5- or 10-cm depth and the TFs obtained by logarithmic interpolation to the desired depth for each core sample. The calculated TFs are given in Appendix B for as many samples as possible. Additionally, TFs for variations of some geometric models are also included in the tables. These variations are as described here.

In Table B1, additional TFs were calculated for:

1. Motoyasu Bridge sample from both the river and the bridge side of the pillar (the bridge side was used),
2. Shirakami Shrine granite with and without a tree foliage cover (5 g cm^{-2}), and
3. City Hall concrete core with and without an extra 0.05 g cm^{-3} of water in the concrete.

There is not much difference in the TFs for both sides of the Motoyasu Bridge pillar. The riverside has a 10% higher TF for thermal neutron activation within the first centimeter depth. The original granite rock calculation at the Shirakami Shrine did not match either the ^{36}Cl or ^{152}Eu activation that was measured in the samples. The measurements dropped off faster with depth than the calculations, as was also noted by Shizuma et al. (1997). The only way found to match the measurements was to cover the granite rock with a neutron moderator. Adding a thick wood cover representing a wood shrine or thick foliage produced better agreement between the measurements and calculations. The moisture in the building concretes in 1945 will never be accurately known. As an illustration of the effect of moisture, adding water to the City Hall concrete (increasing 5.5% water to 7.7%) gave an increase in near-surface thermal activation due to buildup of 5 to 10%. However, at depths beyond 20 cm, the activation decreased by about 25%.

In Table B2, TFs were calculated for several different gravestone geometries:

1. Sample on top surface or on hypocenter-facing side of granite gravestone,
2. Granite gravestone on wet soil or granite surface,

Next Page